Computational modeling of pharmacokinetics and tumor dynamics to guide anti-cancer treatment

Yin, A.

Chapter 6

Population pharmacokinetic and pharmacogenetic analysis of mitotane in patients with adrenocortical carcinoma: towards individualized dosing

Anyue Yin, Madeleine H.T. Ettaieb, Jesse J. Swen, Liselotte van Deun, Thomas M.A. Kerkhofs, Robert J.H.M. van der Straaten, Eleonora P.M. Corssmit, Hans Gelderblom, Michiel N. Kerstens, Richard A. Feelders, Marelise Eekhoff, Henri J.L.M. Timmers, Antonio D'Avolio, Jessica Cusato, Henk-Jan Guchelaar, Harm R. Haak, Dirk Jan A.R. Moes

Clin Pharmacokinet. 2021 Jan;60(1):89-102

Abstract

Background: Mitotane is the only approved treatment for patients with adrenocortical carcinoma (ACC). A better explanation for the variability in the pharmacokinetics (PK) of mitotane, and the optimization and individualization of mitotane treatment, is desirable for patients.

Objectives: This study aims to develop a population PK (PopPK) model to characterize and predict the PK profiles of mitotane in patients with ACC, as well as to explore the effect of genetic variation on mitotane clearance. Ultimately, we aimed to facilitate mitotane dose optimization and individualization for patients with ACC.

Methods: Mitotane concentration and dosing data were collected retrospectively from the medical records of patients with ACC taking mitotane orally and participating in the Dutch Adrenal Network. PopPK modelling analysis was performed using NONMEM (version 7.4.1). Genotypes of drug enzymes and transporters, patient demographic information, and clinical characteristics were investigated as covariates. Subsequently, simulations were performed for optimizing treatment regimens.

Results: A two-compartment model with first-order absorption and elimination best described the PK data of mitotane collected from 48 patients. Lean body weight (LBW) and genotypes of *CYP2C19*2* (rs4244285), *SLCO1B3* 699A>G (rs7311358), and *SLCO1B1* 571T>C (rs4149057) were found to significantly affect mitotane clearance (CL/F), which decreased the coefficient of variation (CV%) of the random inter-individual variability of CL/F from 67.0 to 43.0%. Fat amount (i.e. body weight - LBW) was found to significantly affect the central distribution volume. Simulation results indicated that determining the starting dose using the developed model is beneficial in terms of shortening the period to reach the therapeutic target and limit the risk of toxicity. A regimen that can effectively maintain mitotane concentration within 14–20 mg/L was established.

Conclusions: A two-compartment PopPK model well-characterized mitotane PK profiles in patients with ACC. The CYP2C19 enzyme and SLCO1B1 and SLCO1B3 transporters may play roles in mitotane disposition. The developed model is beneficial in terms of optimizing mitotane treatment schedules and individualizing the initial dose for patients with ACC. Further validation of these findings is still required.

1. Introduction

Adrenocortical carcinoma (ACC) is a rare endocrine malignancy (1 per million per year) with a poor prognosis and limited treatment options [1]. Mitotane, a highly lipophilic compound, is the only treatment approved by the US FDA and the European Medicines Agency for ACC [1]. Mitotane is developed as an orally administered treatment and its absorption is improved by concomitant intake of fat-rich food [2]. The bioavailability of mitotane is around 35–40% [3]. Mitotane has a high volume of distribution and the primary distribution site is fat [3, 4]. The half-life of mitotane elimination ranges from 18 to 159 days, with a median of 53 days [2, 3].

The efficacy and toxicity of mitotane are related to the plasma concentration [1, 3]. In order to ensure efficacy and avoid increased toxicity, the mitotane plasma concentration should be between the therapeutic range of 14 and 20 mg/L, which requires therapeutic drug monitoring (TDM) [1].

However, due to the large distribution volume and long half-life of mitotane, a long-time interval (around 3–5 months [1]) is usually required for patients to reach the effective concentration [3], which limits the clinical utility of mitotane. The inability to reliably predict mitotane plasma concentrations may result in a prolonged time to reach the target value, hence causing a significant delay in tumour treatment, or may give rise to drug toxicity. In addition, it has been demonstrated that only half of the patients who received a high-dose regimen for 3 months achieved the target [5], suggesting a demand for individualized treatment and a presence of high inter-individual variability (IIV) in the pharmacokinetics (PK) of mitotane. Currently, the dosage titration is largely expert-based, making it prone to errors. Therefore, a tool enabling mitotane concentration prediction and an optimized treatment regimen for individual patients, which shortens the period required to reach the target concentration while limiting the toxicity, would be desirable for patients with ACC.

A population PK (PopPK) modelling approach with mixed-effect models enables quantitative characterization and prediction of drug PK profiles for both the study population and individuals [6]. The development of a PopPK model of mitotane would be beneficial for the characterization and understanding of mitotane PK, as well as for the optimization and personalization of mitotane treatment. Until now, two studies have performed PopPK modelling analysis on mitotane in patients with ACC [3, 7]; one-compartment models were developed in these two studies. One study assuming a self-induced clearance and a body mass index (BMI) was found to be a covariate of mitotane distribution volume [3], while the other study identified the effects of triglyceride and high-density lipoprotein on mitotane clearance [7]. Another model-based PK study of mitotane developed a three-

compartment model and showed weak correlations of age, sex, body weight, height, and body surface area with model parameters [8].

In order to further elucidate the variability of mitotane PK, it would be beneficial to explore the effect of pharmacogenetic polymorphisms [8]. Although the exact PK pathway of mitotane and the enzymes involved in mitotane metabolism remain unknown [9], two studies suggested possible roles for cytochrome P450 (CYP) 2B6 and CYP2C9 [10, 11]. One study demonstrated that the genotype of *CYP2B6*6* (rs3745274) was significantly correlated with mitotane plasma concentrations at 3 and 6 months after the initiation of treatment [10]. The other study showed that one patient with high mitotane concentration was a CYP2C9 intermediate metabolizer [11]. Further analysis of the relationship between genes encoding for PK enzymes and transporters and mitotane PK profiles, and incorporating these variables into a PopPK model, may allow better explanation of mitotane PK variability.

In the current study, a PopPK analysis was performed for mitotane in patients with ACC utilizing the retrospectively collected PK data. The effect of genes encoding drug absorption, distribution, metabolism, and elimination (ADME), patient demographic information, and clinical characteristics on mitotane PK were investigated as covariates. We aimed to develop a PopPK model to describe and predict the PK of mitotane in patients with ACC, as well as to explore the effect of genetic variation on mitotane clearance. Moreover, we intended to better explain mitotane PK variability using the developed model and to facilitate treatment optimization and individualization for patients with ACC.

2. Methods

2.1 Patients

Forty-nine adult patients diagnosed with ACC (≥18 years old), who were enrolled in the Dutch Adrenal Network Registry, had been treated with mitotane, had provided consent, and had available mitotane dosing information as well as concentration data were included in this PopPK analysis. One patient was eventually excluded because of missing information regarding starting dose.

The study was approved by the Medical Ethical Committee of the Máxima Medical Center, Veldhoven (2015), and approval for the inclusion of patients in other institutes was obtained from the local boards. The required informed consents were obtained from all patients. All procedures performed in this study were in accordance with the ethical standards of the institutional Medical Ethical Committee and the 1964 Helsinki Declaration.

2.2 Pharmacokinetic (PK) data

Data on mitotane plasma concentrations, including concentrations from routine TDM, data sampled during one treatment interval, and data collected after treatment discontinuation, as well as all mitotane dosing data, were collected retrospectively from patients' medical records. Patients administrated mitotane orally were advised to take mitotane with fat-rich food. Concomitant medication information was not included in the current analysis since the data were not complete. The mitotane plasma concentrations were determined by a validated gas-chromatography/ mass spectrometry assay at the Department of Clinical Pharmacy and Toxicology, Leiden University Medical Center (LUMC) [12]. The lower limit of quantification (LLOQ) was 2 mg/L. In addition, patients' demographic information, including age, sex, and body weight (WT) and height (HT) at the start of treatment, were collected. Furthermore, levels of serum aspartate transaminase (ASAT), alanine transaminase (ALAT), gamma-glutamyltransferase (γGT), total cholesterol, and estimated glomerular filtration rate (GFR; recorded as 0 if the result was ≥ 60 mL/min/1.73 m^2, otherwise 1) were also collected in our analysis.

Lean body weight (LBW) and fat amount (FAT) were also calculated for each patient. LBW was estimated using the *Boer* formula [13] and FAT was obtained by subtracting LBW from WT.

2.3 Genotyping method

The DNA of included patients was isolated from EDTA blood samples using Maxwell (Promega, Leiden, The Netherlands) or MagNAPure compact (Roche, Almere, The Netherlands). Genotyping of patients was performed using the Drug Metabolizing Enzymes and Transporters (DMET™) Plus array (Affymetrix UK Ltd, High Wycombe, UK), which contains 1936 genetic variants (1931 single nucleotide polymorphisms [SNPs] and 5 copy number variations [CNVs]) of ADME-related enzymes and transporters [14], according to the manufacturers' protocol. The method has been previously described in detail [15, 16].

A preset selection was performed using the DMET™ console software that generates fully annotated marker reports based on a translation file as recommended by Affymetrics® [17]. The reports include commonly recognized, haplotype-based allele calls commonly cited in Medline reference studies [18-20]. The DMET™ Plus allele translation software produces a comprehensive genotyping report containing pharmacogenomic reference data on all probes. This step leads to the selection of 959 SNPs from the total of 1931 SNPs present on the DMET™ platform. Subsequently, the SNPs that deviated from Hardy-Weinberg equilibrium ($p < 0.0001$), with a call rate below 97% or with a minor allele frequency

(MAF) < 0.1, as well as tri-allelic SNPs and SNPs of genes located on the X chromosome, were excluded from further analysis.

2.4 Population PK model development

Based on the obtained mitotane concentration data, a non-linear mixed-effects model was developed. Parameters were estimated using the first-order conditional estimation method with interaction (FOCEI) implemented in NONMEM software version 7.4.1 (ICON Development Solutions, Ellicott City, MD, USA). One-, two- and three-compartment models with first-order absorption and first-order elimination were explored as the structural model. Data points below the LLOQ were omitted since they only contributed to 3.6% of the observations [21, 22].

Since the majority of collected data were trough concentrations, and data regarding the absorption phase were limited, the absorption rate constant (KA) was first estimated based on a sub-dataset containing data of the patients who contributed multiple data points during one treatment interval at steady state. The KA estimate was then fixed to analyze the full dataset. Inter-occasion variability (IOV) was incorporated on apparent systemic clearance (CL/F) and every 200 days of treatment was defined as an occasion. In addition, to simplify the situation, all patients were assumed to receive a single dose once daily at 8:00 am, with the dose amount being equal to the total daily dose.

A further detailed description of the PopPK modelling methods is shown in **Online Resource 6.1**.

2.5 Identify potential correlated single nucleotide polymorphisms and covariate analysis

Since knowledge regarding the relationship between mitotane clearance and pharmacogenetic polymorphisms is limited, an exploratory analysis was first performed to find potential SNPs that were correlated with mitotane clearance. The estimates of random IIV of CL/F (η_{IIVi_CL}) from the basic model and the genotyping results were utilized. For each SNP, when the number of patients in a minor homozygous group was < 4, the results of these patients were combined with the corresponding heterozygote group for the association analysis assuming a dominant allele effect. Additionally, when the number of patients with genotype results of 'zero copy number' or 'possible rare allele' was less than four, or when patients had 'NoCall' results, the results were not included for statistical analysis. A one-way analysis of variance (ANOVA) test and a two-sided *t* test were performed

using R version 3.6.1 (The R Foundation for Statistical Computing Vienna, Austria) to evaluate the difference in η_{IIVi_CL} across genotype groups for each SNP. Selection of the test method depended on the number of genotype groups of each SNP after the combination. The SNPs were considered to correlate with mitotane clearance if the p-value was < 0.05. Correction for multiple testing was not performed due to the exploratory characteristics of the current analysis.

The identified SNPs, as well as patient demographic information and clinical characteristics, were considered in the covariate analysis. The stepwise covariate modelling (SCM) function implemented with Perl-Speaks-NONMEM (version 4.7.0) [23] was applied. Both forward inclusion ($p < 0.05$) and backward elimination processes ($p < 0.01$) were performed to identify significant covariates. A more detailed description of the covariates analysis is shown in **Online Resource 6.1**.

2.6 Model evaluation

The predictability and stability of the final model was evaluated using goodness-of-fit (GOF) plots, prediction-corrected visual predictive checks (pcVPC) [24], and non-parametric bootstrap. Normalized prediction distribution errors (NPDEs) were also applied for evaluation. All figures were created using R (The R Foundation for Statistical Computing). A detailed description of the evaluation methods is shown in **Online Resource 6.1**.

2.7 Simulations for treatment optimization

Based on the final model, simulations were performed to optimize mitotane dosing regimen and starting dose determination, in order to shorten the target-reaching time while limiting the risk of toxicity. The simulation was performed for patients included in this study, as they are considered to be able to represent the corresponding adult patient population. The individual parameters of each patient were used to simulate the 'real' mitotane concentrations (C_{sim_real}) under each regimen. The residual errors were not considered. Different strategies of adjusting the dose according to C_{sim_real} are shown in **Figure 6.1**. All simulations were performed using R (The R Foundation for Statistical Computing) and the differential equations were solved using the RxODE package (version 0.6-1) [25]. A detailed description of the regimens and simulation methods are shown in **Online Resource 6.1**.

On the basis of the simulated PK curves, for patients who originally reached the target, the mean and maximum time needed to reach the target (T_{target}, the first day when $C_{sim\_real} \geq 14$ mg/L), the mean percentage of days when C_{sim_real} was higher than 20 mg/L in the first 200 days ($P_{toxicity}$), and the mean percentages of C_{sim_real} located outside the thera-

a Regimen 1

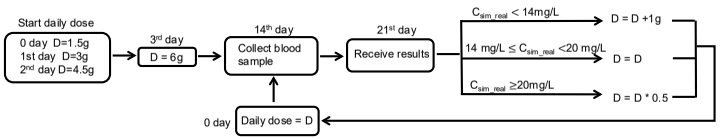

b Regimen 2-2g, 2-4g, and 2-6g

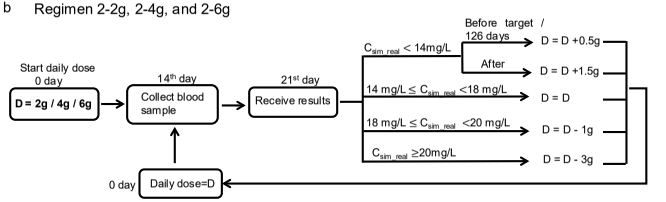

c Regimen 3-77day, 3-98day, and 3-119day

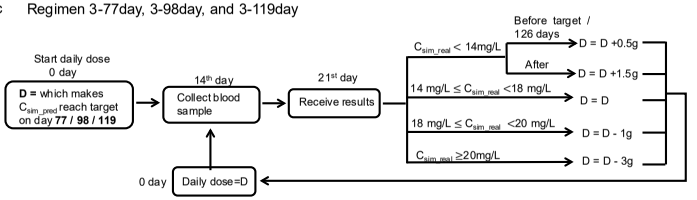

d Regimen 4-(-4g), 4-(50%), 5-(-4g), 5-(50%)

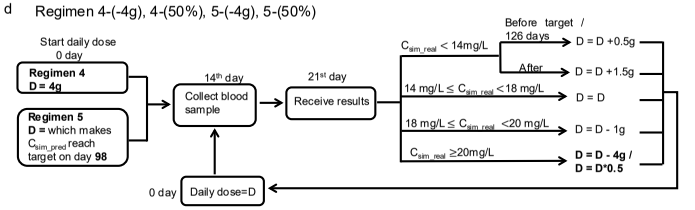

e Regimen 6-1, 6-2, 7-1, and 7-2

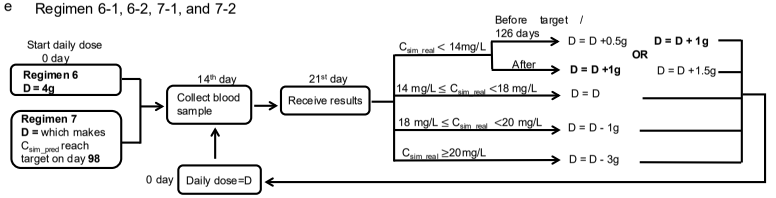

f Regimen 8

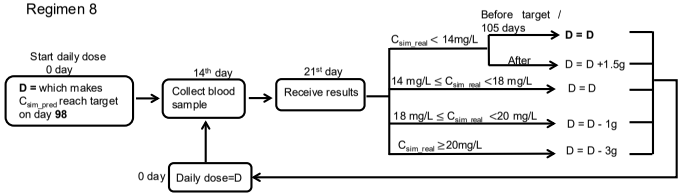

g Regimen 9

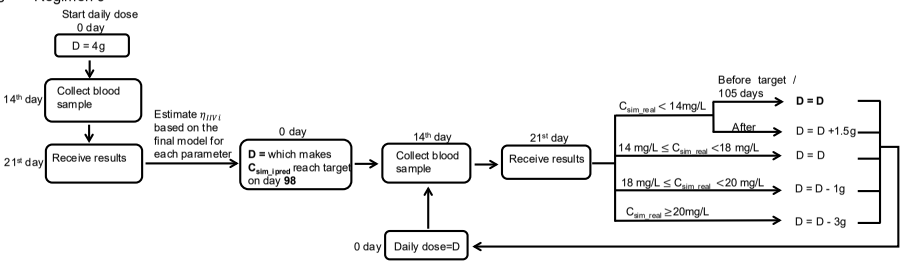

Figure 6.1: Designed treatment regimens that were evaluated by simulation. **(a)** A previously reported dosing regimen (Regimen 1), where the dose started as 1.5 g/day and increased up to 6 g/day in 4 days and continued until the next dose adjustment. The dosage was adjusted each time according to the monitored mitotane concentration level. **(b)** Regimens where all patients started with 2 g (Regimen 2–2 g), 4 g (Regimen 2–4 g) or 6 g (Regimen 2–6 g) per day. Dosage increased by 0.5 g every 21 days till the target was reached or 126 days if C_{sim_real} < 14 mg/L. Thereafter, the dosage increased by 1.5 g if C_{sim_real} < 14 mg/L, remained unchanged if 14 mg/L ≤ Csim_real < 18 mg/L, decreased by 1 g if 18 mg/L ≤ C_{sim_real} < 20 mg/L, and decreased by 3 g if C_{sim_real} ≥ 20 mg/L. **(c)** Regimens where patients started with an individualized dose that allowed C_{sim_pred} on day 77 (Regimen 3–77 day), 98 (Regimen 3–98 day), or 119 (Regimen 3–119 day) reach the target. The remaining dose-adjustment strategies were the same as Regimen 2. **(d)** Regimens where patients started with 4 g/day (Regimen 4) or an individualized dose (Regimen 5) and the dosage decreased by 4 g, or 50%, if C_{sim_real} ≥ 20 mg/L. The remaining dose-adjustment strategies were the same as Regimen 2. **(e)** Regimens where patients started with 4 g/day (Regimen 6) or an individualized dose (Regimen 7) and the dosage increased by 1 g after reaching target or 126 days if C_{sim_real} < 14 mg/L (Regimen 6–1 and 7–1), or increased by 1 g until reaching target or 126 days if C_{sim_real} < 14 mg/L (Regimen 6–2 and 7–2). The remaining dose-adjustment strategies were the same as Regimen 2. **(f)** A regimen where patients started with an individualized dose that remained unchanged until reaching target or 105 days if C_{sim_real} < 14 mg/L. The remaining dose-adjustment strategies were the same as Regimen 2. **(g)** A regimen where patients started with 4 g/day for the first 21 days and the next dosage was determined that allowed C_{sim_ipred} on day 98 to reach the target (Regimen 9). The remaining dose-adjustment strategies were the same as Regimen 8. C_{sim_real}, simulated 'real' mitotane concentrations based on individual parameters, C_{sim_pred}, model predictions based on patient characteristics, C_{sim_ipred}, model predictions using individual parameters, i.e. incorporating the inter-individual variability (η_{IIVi}) estimated based on the first monitored concentration.

peutic window after reaching the target ($P_{o.window}$), were calculated and compared across different strategies. $P_{toxicity}$ represents the probability of causing toxicity in the early phase of treatment, and $P_{o.window}$ represents the ability to maintain the concentration within the therapeutic window. Meanwhile, the median maximum and minimum C_{sim_real}, as well as the range of determined starting doses, were also collected and evaluated. As an optimized regimen is expected to be able to ensure a shorter target-reaching time and well-maintain the concentration within the therapeutic window while not causing much toxicity, the optimization target was defined as the mean T_{target} ≤ 90 days (3 months), the mean $P_{toxicity}$ ≤ 10%, and the mean $P_{o.window}$ ≤ 15%.

Using the optimized regimen, a Shiny application was created based on the Shiny package (version 1.4.0) and the RxODE package in R (The R Foundation for Statistical Computing) in order to perform simulation for a random patient and to elucidate an option of providing treatment advice for a new patient based on the model. A detailed description is shown in **Online Resource 6.2**.

3. Results

3.1 Patients and data

Data from 48 patients with ACC (21 males and 27 females) were included in the PopPK analysis. The characteristics of patients are summarized in **Table 6.1**. Patients received mitotane treatment between 2002 and 2017, and the median duration of treatment was 713.5 days (range 90–2856). The total daily dosage ranged from 0.5 to 16 g/day and was divided into one to four doses. Five (two patients), six (one patient), and eight (one patient) daily dosages were also applied occasionally. Forty-one patients reached the concentration target during treatment, among whom 16 patients reached the target after 150 days. In total, 914 concentration data points were collected from patients' electronic hospital records,

Table 6.1: Patient characteristics (n = 48)

Characteristic	Value/mean	SD	Range
Patient characteristics			
No. of patients	48		
Sex, male [n (%)]	21 (43.8)		
Age, years[a]	52.0	12.1	22.6–76.8
Weight, kg[a] (n = 2 no record)	80.0	15.9	52.5–120
Height, cm[a] (n = 5 no record)	172	10.0	154–193
BMI, kg/m^2[a] (n = 5 no record)	27.1	4.48	18.2–38.3
LBW, kg[a] (n = 5 no record)	55.8	10.0	39.7–78.5
ASAT, IU/L[b] (n = 1 no record)	45.15	35.3	16–185
ALAT, IU/L[b] (n = 1 no record)	42.68	35.6	9–197
γGT, IU/L[b] (n = 1 no record)	278.70	215.9	55–898
GFR, > 50% of records were normal [n (%)] (n = 7 no record)	39 (95.1)		
Cholesterol, mmol/L[b] (n = 11 no record)	6.54	1.56	3.6–11.6
Disease characteristics [n (%)]			
ENSAT I, patients	2 (4.2)		
ENSAT II, patients	19 (39.6)		
ENSAT III, patients	10 (20.8)		
ENSAT IV, patients	17 (35.4)		
Target-reaching characteristics			
No. of patients who reached the target	41		
150 days [n (%)]	16 (39.0)		
≤ 90 days [n (%)]	19 (46.3)		
Target-reaching time, days	142	113.9	24–579
Duration of treatment, days	742	553.2	90–2856

SD, standard deviation; BMI, body mass index; LBW, lean body weight; ASAT, aspartate transaminase; ALAT, alanine transaminase; γGT, gamma-glutamyl transferase; GFR, glomerular filtration rate; ENSAT, European Network for the Study of Adrenal Tumors.

[a] At the start of treatment.

[b] Mean record of each patient.

33 of which were below the LLOQ. The time-course of collected mitotane concentrations is shown in **Figure 6.2**. Nine patients contributed multiple sampling data within one treatment interval and 13 patients had more than one data point collected after treatment discontinuation. The median number of data points contributed by each patient was 16.5, ranging from 2 to 47.

Data from 48 patients with ACC (21 males and 27 females) were included in the PopPK analysis. The characteristics of patients are summarized in **Table 6.1**. Patients received mitotane treatment between 2002–2017 and the median duration of treatment was 713.5 days (range from 90–2856 days). The total daily dosage ranged from 0.5–16 g per day and was divided into one to four doses. Five (2 patients), six (1 patient), and eight (1 patient) daily dosages were also applied occasionally. Forty-one patients reached the concentration target during treatment, among whom 16 patients reached the target after 150 days. In total, 914 concentration data points were collected from patients' electronic hospital records, 33 of which were below the LLOQ. The time-course of collected mitotane concentrations was shown in **Figure 6.2**. Nine patients contributed multiple sampling data within one treatment interval and 13 patients have more than one data point collected after treatment discontinuation. The median number of data points contributed by each patient was 16.5, ranging from 2 to 47.

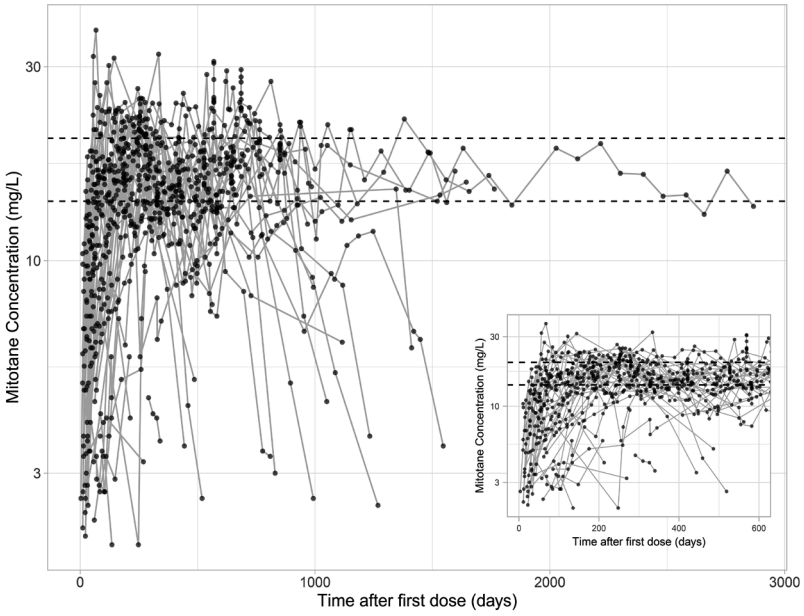

Figure 6.2: Mitotane concentration-time curve collected from patients on logarithmic scale. Inserts show the data during the first 600 days of treatment.

3.2 The basic model

Based on the sub-dataset containing data from the nine patients with multiple sampling data within one treatment interval, the KA was estimated as 22.1 (/day) and 15.0 (/day) under a one-compartment and a two-compartment model structure, respectively. A three-compartment model could not be identified, since (1) the time-course of mitotane concentration did not meet the characteristics of a three-compartment model; and (2) when running the three-compartment model, the parameters were shown to be unidentifiable. The basic models were then developed by fitting the full dataset with fixed KA and incorporating IOV on CL/F. The relative standard error (RSE) parameter estimates of both two-model structures were all within the acceptable range (< 30%). The objective function value (OFV) of the two-compartment model was reduced by 92.13 compared with that of the one-compartment model ($p < 0.001$, degree of freedom = 4), suggesting an improvement on the model fitness. Therefore, the two-compartment model was ultimately selected for describing mitotane PK profiles in patients with ACC in this study. The model structure is shown in **Online Resource 6.1**, **Figure S6.1**. The parameter estimates of the basic model are shown in **Table 6.2**. The high percentage coefficient of variation (CV%) of IIV for all parameters was identified, and the CV% of IIV for the apparent distribution rate constant (Q/F) was even higher than 100%.

3.3 Pharmacogenetic analysis

For each patient, the genotyping results of the 959 SNPs from the DMET™ platform were obtained. A list of these SNPs can be found in **Online Resource 6.3**. All SNPs were in Hardy–Weinberg equilibrium ($p \geq 0.0001$). A flow diagram of the selection of genetic variants is shown in **Figure 6.3**. Eventually, 172 SNPs were included for further investigation. Among these 172 SNPs, 55 had less than four patients belonging to the minor homozygous group. The 'NoCall' result was reported in one patient in 19 SNPs and the 'Possible Rare Allele' result was reported in one patient in one SNP. The results of these patients were thus not included in the association analysis of corresponding SNPs. In contrast, the 'Zero Copy Number' result occurred in three SNPs in 8, 24, and 24 patients, respectively. Thus, patients with a 'Zero Copy Number' were treated as a different genotype group in the association analysis of these three SNPs.

Finally, the result of the association test showed that 11 SNPs, as shown in **Online Resource 6.1**, **Table S6.1**, were potentially related to mitotane clearance ($p \leq 0.05$). Among these 11 SNPs, the genotyping results of *CYP2C18* 1154C>T (rs2281891) and *CYP2C19*2* (rs4244285) were shown to be 100% in linkage disequilibrium in our dataset, which was the same as the genotyping results of *SLCO1B3* 334G>T (rs4149117), 699A>G (rs7311358),

Table 6.2: Parameter estimates of both the basic and final models

Parameters	Basic model			Final model			Bootstrap	
	Estimate	IIV (CV%)	IOV[c]	Estimate	IIV (CV%)	IOV[c]	Median	95% CI
	(RSE%)	[shrinkage, %]	(CV%)	(RSE%)	[shrinkage, %]	(CV%)		
KA (/day)	15.0 fixed	-	-	15.0 fixed	-	-	15	-
CL/F (L/day)[a]	217 (11)	67.0 [8]	30.5	298 (13)	43.0 [16]	31.6	281.6	200.5–398.4
CL_SNP1 (GA/AA)	-	-	-	0.551 (15)	-	-	0.573	0.385–0.881
CL_SNP2 (AG/GG)	-	-	-	0.601 (19)	-	-	0.613	0.419–0.949
CL_SNP3 (CC)	-	-	-	0.753 (10)	-	-	0.784	0.550–1.07
CL_SNP3 (TT)	-	-	-	2.49 (29)	-	-	2.67	0.991–6.16
CL_LBW (power)	-	-	-	1.10 (16)	-	-	1.07	0.205–2.13
V_c/F (L)[b]	4790 (20)	68.1 [53]	-	6210 (18)	47.2 [55]	-	6795	3281–10752
V_c_FAT (power)	-	-	-	1.22 (19)	-	-	1.29	0.450–2.18
V_p/F (L)	19300 (13)	76.9 [17]	-	18100 (12)	88.8 [15]	-	17882	11341–25709
Q/F (L/day)	1100 (21)	102 [34]	-	883 (20)	97.3 [34]	-	785.4	337.4–1502
Residual errors								
PRO (CV%)	16.6 (7)	-	-	16.6 (6)	-	-	16.8	14.2–18.9
ADD (mg/L)	0.931 (28)	-	-	0.920 (17)	-	-	0.871	0.373–1.384

SNP1: *CYP2C19*2* (rs4244285); *SNP2*: *SLCO1B3* 699A>G (rs7311358); *SNP3*: *SLCO1B1* 571T>C (rs4149057); LBW, lean body weight; FAT, fat amount; RSE, relative standard error; CV, coefficient of variation; IIV, interindividual variability; IOV, interoccasion variability; PRO, proportional residual error; ADD, additive residual error; CL/F, apparent system clearance; KA, absorption rate constant; V_c/F, apparent distribution volume of central compartment; V_p/F, apparent distribution volume of peripheral compartment; Q/F, apparent distribution rate constant; CI, confidence interval

[a] $CL/F = CL/F_t * CL\_SNP1 * CL\_SNP2 * CL\_SNP3 * (\frac{LBW}{56.6})^{CL\_LBW}$

[b] $V_c/F = V_c/F_t * (\frac{FAT}{23.6})^{Vc\_FAT}$

[c] Every 200 days of dosing was defined as an occasion.

and 1557G>A (rs2053098) and that of the three SNPs located on *VKORC1* (283+124G>C, 174-136C>T, and -1639G>A). The results of the 11 identified SNPs were subsequently combined into the full dataset for stepwise covariate analysis.

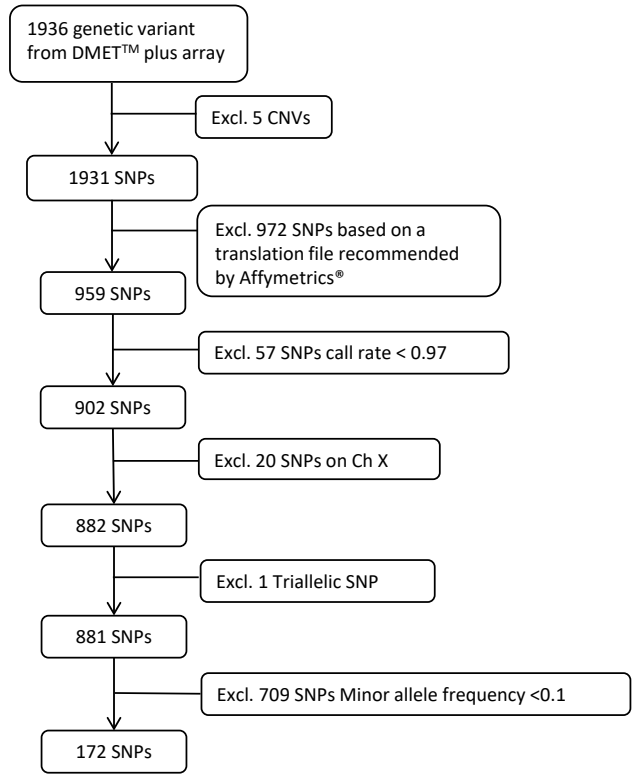

Figure 6.3: Selection of the genetic variants. Excl. excluding, Ch X chromosome X, DMET™ Drug Metabolizing Enzymes and Transporters, CNVs copy number variations, SNPs single nucleotide polymorphisms.

3.4 The final model

The parameter estimates of the final model are shown in **Table 6.2**. The *CYP2C19*2* (rs4244285), *SLCO1B3* 699A>G (rs7311358), and *SLCO1B1* 571T>C (rs4149057) genotypes, and LBW at the start of treatment, with power relation, were found to have a significant effect on the CL/F of mitotane (**Table 6.2**). Carrying the 'A' variant in *CYP2C19*2* reduced the CL/F by 44.9%, and carrying 'G' variant in *SLCO1B3* 699A>G resulted in a 39.9% reduction in CL/F (**Table 6.2**). As for *SLCO1B1* 571T>C, the CL/F of patients carrying one 'C' variant decreased to 40.2% that of wild-type patients, while the CL/F of patients carrying two 'C' variants decreased to 30.2%. The distribution of η_{IIVi_CL} derived from the basic model in each genotype group of the above three SNPs is shown in **Online Resource**

6.1, **Figure S6.2**. In addition, FAT at the start of treatment with power relation was found to significantly influence the apparent distribution volume of the central compartment (V_c/F). The inclusion of these covariates decreased the CV% of CL/F and V_c/F from 67.0% and 68.1% to 43.0% and 47.2%, respectively. Overall, the parameter estimates were shown to be in good agreement with the bootstrap results (**Table 6.2**).

The GOF plots (**Figure 6.4**) show that the individual predictions of the final model are in good accordance with the observations, while the population predictions are slightly deviated from the observations. The conditional weighted residual errors (CWRES) randomly distributed around zero, without obvious trends over time or across population predictions. The pcVPC plot (**Figure 6.5**) shows that the 5th, 50th, and 95th percentiles of

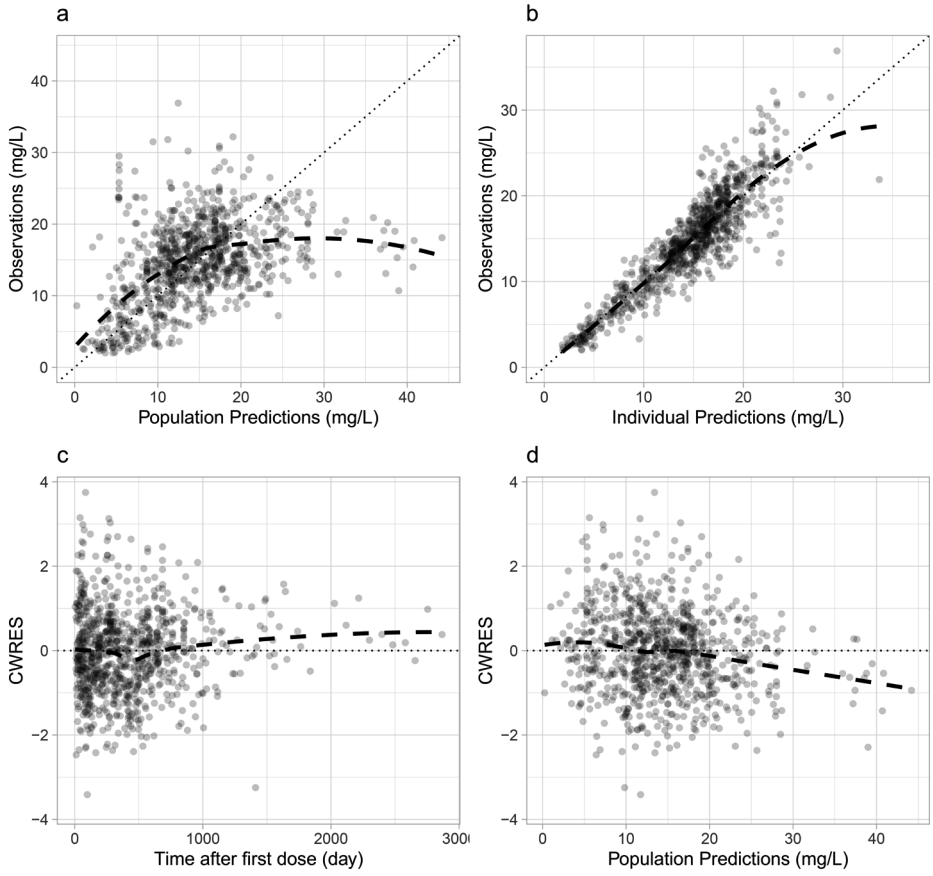

Figure 6.4: Goodness-of-fit plots of the final population pharmacokinetic model of mitotane in patients with adrenocortical carcinoma, including observations versus **(a)** population predictions and **(b)** individual predictions, and CWRES versus **(c)** time and **(d)** populations predictions. The *black dotted lines* represent *y = x* (**a, b**) and *y = 0* (**c, d**), and the *black dashed lines* represent the corresponding LOESS regressions. CWRES; conditional weighted residual errors; LOESS, locally estimated scatterplot smoothing.

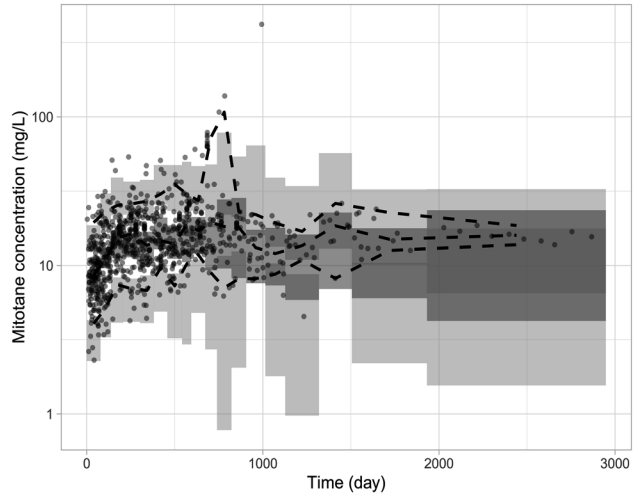

Figure 6.5: Prediction-corrected visual predictive check plot of the final model on the logarithmic scale. *Black dashed lines* represent the 50th, 95th and 5th percentiles of the prediction- corrected observations; *light-grey shading* represents the 95% confidence interval of the 95th and 5th percentiles of the simulations; and *dark-grey shading* represents the 95% confidence interval of the 50th percentiles of the simulations.

prediction-corrected concentrations can be mostly adequately covered by the 95% confidence interval (CI) of the corresponding percentiles of simulations, although a few large prediction-corrected concentrations are present. The NPDE results are shown in **Online Resource 6.1**, **Figure S6.3**.

3.5 Simulation results

The simulation results of different regimens in included patients who originally reached the target (n = 41) are summarized in **Table 6.3**.

The previously suggested high-dose regimen (Regimen 1) resulted in the lowest T_{target} but the highest $P_{toxicity}$. The C_{sim_real} can also not be well-maintained within the therapeutic range.

As for the newly designed strategies, if all patients started with the same dosage (Regimen 2–2 g, 2–4 g and 2–6 g), the increase in the starting dosage reduced the T_{target} but increased $P_{toxicity}$ and weakened the ability of maintaining C_{sim_real} within the therapeutic range. When determining the starting dose individually (Regimen 3–77 day, 3–98 day and 3–119 day), Regimen 3–98 day fulfilled the optimization target and resulted in a lower T_{target} but higher $P_{toxicity}$ and $P_{o.window}$ compared with Regimen 2–4 g. The range of determined starting dose was in accordance with what is currently recommended [26] (**Table 6.3**).

Table 6.3: Simulation results of different treatment regimens for included patients who originally reached the target (n = 41)

Regimen (Figure 6.1)	Mean T_{target} (day)	Max T_{target} (day)	Mean $P_{toxicity}$ (%)	Mean $P_{o.window}$ (%)	Median max / min C_{sim_real} (mg/L)	Starting dose range (g)	
1	54.22	125	23.6	18.35	22.3 / 13.11	-	
2–2 g	133.98	236	4.16	12.6	20.65 / 13.14	2	
2–4 g	89.8	182	7.01	13.15	20.90 / 13.20	4	*
2–6 g	60.61	149	13.85	15.13	21.13 / 13.09	6	
3–77 day	73	173	10.63	12.7	21.07 / 13.29	3.5–7	
3–98 day	85.07	182	9.26	14.35	21.03 / 13.16	3–6	*
3–119 day	97.9	191	6.44	12.22	20.96 / 13.21	2.5–5	
4–(-4 g)	89.8	182	5.96	12.66	20.91 / 13.22	4	*
4–50%	89.8	182	8.82	12.37	20.91 / 13.22	4	*
5–(-4 g)	85.07	182	7.92	13.01	20.84 / 13.14	3–6	*
5–50%	85.07	182	11.13	12.21	20.84 / 13.22	3–6	
6–1	91.12	194	6.61	13.37	20.84 / 12.91	4	
6–2	74.32	151	14.34	16.26	21.57 / 13.02	4	
7–1	86.12	194	8.52	14.69	21.03 / 12.96	3–6	*
7–2	80.27	160	14	15.53	21.46 / 12.87	2.5–5	
8	87.85	191	5.05	11.26	20.34 / 13.30	3.5–7	*
9	87.8	161	5.56	10.72	20.33 / 13.09	3–10	*

T_{target}, target reaching time (the day when simulated mitotane concentration ≥ 14 mg/L), $P_{toxicity}$, percentage of days when simulated mitotane concentrations were higher than the upper limit of mitotane therapeutic window (20 mg/L) in the first 200 days, $P_{o.window}$, percentage of simulated mitotane concentrations located outside the therapeutic window after reaching the target, max maximum, min minimum, * indicates the regimen fulfills the optimization target, C_{sim_real} simulated 'real' mitotane concentrations based on individual parameters.

Compared with Regimens 2–4 g and 3–98 day, increasing the dose reduction amount to 4 g when C_{sim_real} > 20 mg/L reduced the $P_{toxicity}$ and $P_{o.window}$, whereas setting a 50% deduction when C_{sim_real} > 20 mg/L reduced the $P_{o.window}$ but increased the $P_{toxicity}$ (Regimen 4 and 5). Both of these changes did not affect T_{target}. In contrast, when adjusting the dose change amount when C_{sim_real} < 14 mg/L, the evaluated regimens did not provide better results (Regimens 6 and 7).

Regimen 8, where a constant starting dose determined by the model was applied, provided generally better results compared with starting with 4 g/day for all patients (Regimen 2–4 g) in terms of T_{target}, $P_{toxicity}$, and the ability to maintain concentration within the therapeutic range. The suggested starting dose range (3–7 g, median 5 g) was slightly beyond the current recommended range but was considered to be acceptable. In comparison, when determining a constant dose using individual PK parameters (incorporating IIV estimates) [Regimen 9], the $P_{o.window}$ and maximum T_{target} decreased. Although $P_{toxicity}$ increased, it was

still low enough. The suggested doses under Regimen 9 were relatively higher (3–10 g) since IIV was taken into account.

Overall, Regimens 2–4 g, 3–98 day, 4–(-4 g), 4–(-50%), 5–(-4 g), 7–1, 8, and 9 fulfilled the optimization target. The individualized starting dose resulted in a lower T_{target} but higher $P_{toxicity}$ compared with the fixed starting dose. Regimens 3–98 day and 5–(-4 g) provided the lowest mean T_{target}, while regimen 5–(-4 g) resulted in lower $P_{toxicity}$. Regimen 8 provided the lowest $P_{toxicity}$ and Regimen 9 provided the lowest maximum T_{target} and mean $P_{o.window}$. Based on these results, Regimen 5–(-4 g) and Regimen 8 were considered to be more beneficial, while Regimen 9 could also be applied, considering the patients' tolerance to the level of dose increase.

The Shiny app was established based on the final model, and the treatment strategy 5–(– 4 g) was applied since this regimen provided the lowest mean T_{target}. A reduced model where the effect of pharmacogenetic variation was not included was also built in to serve as an alternative option for patients when genotyping results were not available. The results are shown in **Online Resource 6.2**.

4. Discussion

In the current study, a two-compartment PopPK model was developed that adequately described the PK profile of mitotane in patients with ACC. The covariates identified explained 24% and 20.9% of random variability in mitotane clearance and distribution volume, respectively. As mitotane distributes in most body tissues, predominantly in the fat [1], the two-compartment model structure is considered to also be in line with the PK characteristics of mitotane, although the wide 95% CI of the Q/F parameter still indicates uncertainty in the estimation. A three-compartment model structure, which has been previously applied on mitotane [8], could not be identified in this study as the time-course of mitotane concentration did not meet the characteristics of a three-compartment model and parameter estimates for the three-compartment model were found to be unidentifiable.

Because of the limited data in the absorption phase, KA was first estimated based on a sub-dataset and then fixed to analyze the full dataset. Precise KA estimation was unidentifiable if estimating based on the full dataset. The estimates of V_c/F and V_p/F were relatively large, which is in accordance with previous reports and the fact that mitotane distributes in many body tissues [1, 3]. The separate effects of LBW and FAT on mitotane distribution volumes were of interest in this study as they are more realistic covariates physiologically [3, 4]. As a result, FAT was found to be a significant covariate on the V_c/F. The estimated

half-life of mitotane in the included patients ranged from 16.4 to 700.6 days, with a median of 101.5 days. This range is wider than what has been previously reported [1, 2], which may be explained by the larger number of patients included in the current study than in the original study [2]. Incorporating IOV on CL/F in the current study explained the intrasubject variability. The estimates of IOV indicate an overall increasing clearance during the first 500 days, followed by a decrease thereafter (**Online Resource 6.1**, **Figure S6.4**). This dynamic indicates that a self-induction in mitotane clearance, which has been suggested previously [3], may exist temporarily.

For the first time, the current study explored and quantified the potential effect of pharmacogenetic variation on mitotane clearance in patients with ACC. Due to the lack of knowledge regarding the PK pathway of mitotane, a wide range of SNPs from the DMET™ Plus array were considered. However, because of the limited number of patients, it was decided to focus on the SNPs with known functionality by adopting a preset selection [17], although an exploratory analysis based on all genetic variants from the DMET™ Plus array was also performed. The flow diagram of the SNP selection and the nine additional SNPs that are potentially correlated to mitotane clearance if the preset selection was not considered are shown in **Online Resource 6.1**, **Table S6.2** and **Figure S6.5**. Genes located on the X chromosome were excluded since only the general influence of sex on mitotane PK was considered.

Eventually, three SNPs, i.e. *CYP2C19*2* (rs4244285), *SLCO1B3* 699A>G (rs7311358), and *SLCO1B1* 571T>C (rs4149057), were included in the final model and were considered as the pharmacogenetic polymorphisms that should be considered for mitotane dose selection. This result also suggests that the CYP2C19 enzyme and SLCO1B3 and SLCO1B1 transporters for drug uptake in the liver might be involved in the mitotane PK pathways, but further confirmation is required.

In fact, in our dataset, *CYP2C19*2* was in 100% linkage disequilibrium with *CYP2C18* 1154C>T (rs2281891), which was the same as *SLCO1B3* 699A>G with *SLCO1B3* 334G>T (rs4149117) and *SLCO1B3* 1557G>A (rs2053098). Comparable high linkage disequilibrium was also found in 1000 Genomes CEU population (Utah residents with Northern and Western European ancestry). Compared with *CYP2C18* 1154C>T, for which no sufficient evidence has been found regarding the effect on the drug PK, the 'A' variant of *CYP2C19** is known to be a nonfunctioning variant and has been demonstrated to decrease the activity of CYP2C19 [27, 28]. Similarly, the variants of *SLCO1B3* 699A>G with *SLCO1B3* 334G>T have been reported to be associated with a decrease in drug clearance, and *SLCO1B3* 699A>G has a stronger level of clinical annotations [29, 30]. Therefore, *CYP2C19*2* and *SLCO1B3* 699A>G were included in the final model.

*CYP2B6*6*, which has been reported to be related to mitotane plasma concentrations detected at 3 and 6 months [10], was not found to have a significant effect on mitotane clearance in the current study. Among the five SNPs located on *CYP2B6* that were included in the association analysis, none were significantly related to mitotane clearance ($p > 0.05$). This discrepancy may be due to the much longer observation period in the present study. One SNP located on *CYP2C9*, *CYP2C9*2* (rs1799853), was also not found to be significant; however, the evidence of the involvement of CYP2C9 is in fact insufficient.

The predictability and stability of the final model were confirmed to be acceptable. In the pcVPC plot, a few prediction-corrected concentrations are inadequately covered by the simulations. A possible explanation is that the observations at corresponding time points are from a single patient and the population prediction of this patient is much smaller than real observations. The deviation of population predictions from observations can also be seen in the GOF plots. Patients' adherence and other unknown factors may also introduce additional bias. Identification of additional covariates, such as the effect of co-medication and food intake, might improve the population predictions.

Based on the final PopPK model, several mitotane treatment strategies were designed and evaluated by simulations. A regimen with a bolus dose followed by a maintenance dose was not considered as this regimen requires a high dosage, which is not tolerable for some patients. Among the regimens that fulfilled the optimization target, applying the individual starting dose determined by the model was demonstrated to shorten the time to achieve the therapeutic window compared with starting with a fixed dose for all patients. Under the setting of individualized starting dose, the regimens with a stepwise increasing dose at start required less time to reach the therapeutic target, while the regimen with a constant starting dose demonstrated the lowest risk of having toxicity. The determined individual starting dose was also acceptable. In addition, the newly designed dose-adjustment strategies were able to satisfactorily keep the mitotane concentrations within the therapeutic range. Therefore, determining the starting dose using the developed model is considered to be most beneficial in terms of shortening the time to reach the therapeutic target and limit the risk of toxicity. However, due to the fact that a shorter T_{target} is normally paired with a higher $P_{toxicity}$, it is suggested to consider, based on a patient's condition, whether the increased risk of having toxicity can be tolerated in order to gain the benefit of a shorter time to reach the therapeutic target when selecting a dosing regimen.

Obtaining individual parameters based on one (or more) TDM result with the PopPK model, and determining the dose amount accordingly, can also decrease the risk of toxicity while providing a satisfactory target reaching time; thus, this is also a promising strategy.

However, patients' tolerance to the high level of dose increase needs to be considered when applying this strategy. This method can also be useful to estimate an adequate dose for the drug concentration level maintenance after reaching the therapeutic window, thereby decreasing the frequency of dose adjustment.

Simulation results also indicate that in order to reduce the risk of having toxicity and to effectively maintain mitotane concentration within the therapeutic range, a better strategy is to set the concentration boundary of dose decreases at 18 mg/L instead of 20 mg/L. This early dose adjustment takes into consideration the 7-day period when the monitoring result is unknown and the dose is not adjusted. The concentration boundary of dose increases needs to be 14 mg/L since it affects the adequacy of maintaining the plasma concentration above 14 mg/L. The frequency of TDM was set at once every 21 days, as suggested by the guideline in the simulation. If TDM is performed less frequently, a larger dose change step will be required.

The current study has some limitations. First, the small number of patients included in this study and the exploratory characteristics of this analysis may influence the power of covariate analysis, especially for pharmacogenetic analysis. However, as the dataset consisted of concentrations on different occasions for each patient, which enabled differentiation between IIV and intrasubject variability (i.e. IOV) in clearance, the certainty of the possible genotype effect on clearance, which is more likely to be covered by IIV since genotype is a constant factor in patients, was increased. Nonetheless, further validation with an external dataset to replicate the findings is warranted to confirm the identified associations and to translate the findings into a clinical recommendation. However, since ACC is a very rare disease (1 per million per year), the collection of another comparable or even larger dataset will be challenging. Therefore, an in vitro assay might be more feasible in future studies to substantiate the activity of the suggested enzymes in mitotane PK. Second, the model lacks a strong ability to accurately predict high concentrations (e.g., peak concentrations) due to the limited data input in the absorption and distribution phase. Furthermore, the accuracy of parameter estimates may be affected by our simplification of multiple daily dosing to a single dose. However, the prediction of mitotane trough concentrations and the suggestion of daily dose based on the model will not be significantly affected. Therefore, we believe this model is still fit for the current application. Third, the impact of coadministrated drugs and food intake on mitotane PK was not taken into account in this study due to the lack of data.

5. Conclusions

The current study presents a two-compartment PopPK model that well-characterizes mitotane PK profiles in patients with ACC. The polymorphisms of *CYP2C19*2* (rs4244285), *SLCO1B3* 699G>A (rs7311358), and *SLCO1B1* 571T>C (rs4149057) were found to be correlated to mitotane PK. Further external or in vitro evaluation is suggested to confirm the results. Moreover, optimized mitotane treatment schedules for patients with ACC were identified by simulation and the developed model can be of help to individualize the initial dose. These strategies should be confirmed in a prospective study

Key points

- A two-compartment population pharmacokinetic (PK) model with first-order absorption and elimination was developed for mitotane based on PK data collected from 48 adrenocortical carcinoma patients.
- The pharmacogenetic variation of *CYP2C19*2* (rs4244285), *SLCO1B3* 699A>G (rs7311358), and *SLCO1B1* 571T>C (rs4149057) was found to have a significant effect on mitotane clearance. Fat amount, which was defined as the difference between total body weight and lean body weight, had a significant effect on the central distribution volume.
- With the help of the model, mitotane treatment can be guided and optimized for individual patients. Further validation of the findings is warranted to confirm the results.

Code availability

PopPK analysis was performed using the FOCEI method implemented in NONMEM software version 7.4.1 (ICONDevelopment Solutions). Statistical analysis, plot generation, and simulations were performed using R version 3.6.1 (The R Foundation for Statistical Computing). The R script of the Shiny application established in this study for simulation can be found at https://github.com/AnyueYin/Shiny-app-script-for-model-simulation---Population-PK-and-PG-analysis-of-mitotane.

References

1. Paragliola RM, Torino F, Papi G, Locantore P, Pontecorvi A, Corsello SM. Role of Mitotane in Adrenocortical Carcinoma - Review and State of the art. Eur Endocrinol. 2018;14(2):62-6. doi:10.17925/EE.2018.14.2.62.
2. Moolenaar AJ, van Slooten H, van Seters AP, Smeenk D. Blood levels of o,p'-DDD following administration in various vehicles after a single dose and during long-term treatment. Cancer Chemother Pharmacol. 1981;7(1):51-4. doi:10.1007/bf00258213.
3. Arshad U, Taubert M, Kurlbaum M, Frechen S, Herterich S, Megerle F, et al. Enzyme autoinduction by mitotane supported by population pharmacokinetic modelling in a large cohort of adrenocortical carcinoma patients. Eur J Endocrinol. 2018;179(5):287-97. doi:10.1530/EJE-18-0342.
4. Vanslooten H, Vanseters AP, Smeenk D, Moolenaar AJ. O,P'-Ddd (Mitotane) Levels in Plasma and Tissues during Chemotherapy and at Autopsy. Cancer Chemoth Pharm. 1982;9(2):85-8. doi:10.1007/bf00265384.
5. Kerkhofs TM, Baudin E, Terzolo M, Allolio B, Chadarevian R, Mueller HH, et al. Comparison of two mitotane starting dose regimens in patients with advanced adrenocortical carcinoma. J Clin Endocrinol Metab. 2013;98(12):4759-67. doi:10.1210/jc.2013-2281.
6. Buil-Bruna N, Lopez-Picazo JM, Martin-Algarra S, Troconiz IF. Bringing Model-Based Prediction to Oncology Clinical Practice: A Review of Pharmacometrics Principles and Applications. Oncologist. 2016;21(2):220-32. doi:10.1634/theoncologist.2015-0322.
7. Cazaubon Y, Talineau Y, Feliu C, Konecki C, Russello J, Mathieu O, et al. Population Pharmacokinetics Modelling and Simulation of Mitotane in Patients with Adrenocortical Carcinoma: An Individualized Dose Regimen to Target All Patients at Three Months? Pharmaceutics. 2019;11(11). doi:10.3390/pharmaceutics11110566.
8. Kerkhofs TM, Derijks LJ, Ettaieb H, den Hartigh J, Neef K, Gelderblom H, et al. Development of a pharmacokinetic model of mitotane: toward personalized dosing in adrenocortical carcinoma. Ther Drug Monit. 2015;37(1):58-65. doi:10.1097/FTD.0000000000000102.
9. Scripture CD, Sparreboom A, Figg WD. Modulation of cytochrome P450 activity: implications for cancer therapy. Lancet Oncol. 2005;6(10):780-9. doi:10.1016/S1470-2045(05)70388-0.
10. D'Avolio A, De Francia S, Basile V, Cusato J, De Martino F, Pirro E, et al. Influence of the CYP2B6 polymorphism on the pharmacokinetics of mitotane. Pharmacogenet Genomics. 2013;23(6):293-300. doi:10.1097/FPC.0b013e3283606cb2.
11. Mornar A, Sertic M, Turk N, Nigovic B, Korsic M. Simultaneous analysis of mitotane and its main metabolites in human blood and urine samples by SPE-HPLC technique. Biomed Chromatogr. 2012;26(11):1308-14. doi:10.1002/bmc.2696.
12. Hermsen IG, den Hartigh J, Haak HR. Mitotane serum level analysis; good agreement between two different assays. Clin Endocrinol (Oxf). 2010;73(2):271-2. doi:10.1111/j.1365-2265.2010.03787.x.
13. Boer P. Estimated lean body mass as an index for normalization of bodv fluid volumes in humans. American Journal of Physiology-Endocrinology and Metabolism. 1984;247(4):F632–6. doi:10.1152/ajprenal.1984.247.4.F632.
14. Arbitrio M, Di Martino MT, Scionti F, Agapito G, Guzzi PH, Cannataro M, et al. DMET (Drug Metabolism Enzymes and Transporters): a pharmacogenomic platform for precision medicine. Oncotarget. 2016;7(33):54028-50. doi:10.18632/oncotarget.9927.
15. Caldwell MD, Awad T, Johnson JA, Gage BF, Falkowski M, Gardina P, et al. CYP4F2 genetic variant alters required warfarin dose. Blood. 2008;111(8):4106-12. doi:10.1182/blood-2007-11-122010.

16. Dumaual C, Miao X, Daly TM, Bruckner C, Njau R, Fu DJ, et al. Comprehensive assessment of metabolic enzyme and transporter genes using the Affymetrix Targeted Genotyping System. Pharmacogenomics. 2007;8(3):293-305. doi:10.2217/14622416.8.3.293.
17. Affymetrix®. White Paper: DMET™ Plus allele translation reports: Summary of comprehensive drug disposition genotyping into commonly recognized allele names 2012 [cited 2020 06 Jan]; Available from: http://tools.thermofisher.com/content/sfs/brochures/dmet_plus_translation.pdf
18. Burmester JK, Sedova M, Shapero MH, Mansfield E. DMET microarray technology for pharmacogenomics-based personalized medicine. Methods Mol Biol. 2010;632:99-124. doi:10.1007/978-1-60761-663-4_7.
19. Sissung TM, English BC, Venzon D, Figg WD, Deeken JF. Clinical pharmacology and pharmacogenetics in a genomics era: the DMET platform. Pharmacogenomics. 2010;11(1):89-103. doi:10.2217/pgs.09.154.
20. Deeken J. The Affymetrix DMET platform and pharmacogenetics in drug development. Curr Opin Mol Ther. 2009;11(3):260-8.
21. Keizer RJ, Jansen RS, Rosing H, Thijssen B, Beijnen JH, Schellens JH, et al. Incorporation of concentration data below the limit of quantification in population pharmacokinetic analyses. Pharmacol Res Perspect. 2015;3(2):e00131. doi:10.1002/prp2.131.
22. Hecht M, Veigure R, Couchman L, CI SB, Standing JF, Takkis K, et al. Utilization of data below the analytical limit of quantitation in pharmacokinetic analysis and modeling: promoting interdisciplinary debate. Bioanalysis. 2018;10(15):1229-48. doi:10.4155/bio-2018-0078.
23. Jonsson EN, Karlsson MO. Automated covariate model building within NONMEM. Pharm Res. 1998;15(9):1463-8. doi:10.1023/a:1011970125687.
24. Bergstrand M, Hooker AC, Wallin JE, Karlsson MO. Prediction-corrected visual predictive checks for diagnosing nonlinear mixed-effects models. AAPS J. 2011;13(2):143-51. doi:10.1208/s12248-011-9255-z.
25. Wang W, Hallow KM, James DA. A Tutorial on RxODE: Simulating Differential Equation Pharmacometric Models in R. CPT Pharmacometrics Syst Pharmacol. 2016;5(1):3-10. doi:10.1002/psp4.12052.
26. Koninklijke Nederlandse Maatschappij ter bevordering der Pharmacie. Mitotaan. 2019 [cited 2019 28 Aug]; Available from: https://kennisbank.knmp.nl/article/Informatorium_Medicamentorum/S1853.html
27. Whirl-Carrillo M, McDonagh EM, Hebert JM, Gong L, Sangkuhl K, Thorn CF, et al. Pharmacogenomics knowledge for personalized medicine. Clin Pharmacol Ther. 2012;92(4):414-7. doi:10.1038/clpt.2012.96.
28. PharmGKB. rs4244285, Variant annotation. [cited 2019 28 Aug]; Available from: https://www.pharmgkb.org/variant/PA166154053/variantAnnotation
29. PharmGKB. rs7311358, Clinical annotation. [cited 2019 28 Aug]; Available from: https://www.pharmgkb.org/variant/PA166154602/clinicalAnnotation
30. PharmGKB. rs4149117, Clinical annotation. [cited 2019 28 Aug]; Available from: https://www.pharmgkb.org/variant/PA166154583/clinicalAnnotation

Online Resource 6.1: Supplementary methods, figures and tables

Supplementary population PK analysis methods

One-, two- and three-compartment models, with first-order absorption and first-order elimination, were explored as the structural model. Relative standard error (RSE) of parameters, which represent the precision of parameter estimates, and the objective function value (OFV) were considered when evaluating the structural models. The one with acceptable RSE and lower OFV was selected as the final basic model structure.

Inter-individual variability (IIV) of parameters were estimated with Eq. 6.1, where P_i represents the parameter of *i*th individual and was assumed to be log-normally distributed, P_t represents typical value of the parameter, and η_{IIV} represents the random IIV which was assumed to be normally distributed with mean of 0 and variance of ω_i^2. In addition, inter-occasion variability (IOV), which reflects the intra-individual variability, of apparent systematic clearance (CL/F) was also included when analyzing the full dataset. As is shown in Eq. S6.1, η_{IOV} represents the random IOV. The distribution of η_{IOV} in each occasion was assumed to be similar and normally distributed with mean of 0 and variance of ω_2^2. In this study, every 200 days of treatment was defined as an occasion as the total observation periods of the patients were long.

The residual error was characterized with a combined proportional and additive model as is shown in Eq. S6.2, where *Obs* represents observations, *IPRED* represents individual predictions, and ε_1 and ε_2 represent the proportional residual error and additive residual error respectively which were assumed to be normally distributed with mean of 0 and variance of σ_1^2 and σ_2^2, respectively.

$$P_i = P_t \cdot e^{\eta_{IIVi}+\eta_{IOVj}} \qquad \text{Eq. S6.1}$$

$$Obs = IPRED \cdot (1 + \varepsilon_1) + \varepsilon_2 \qquad \text{Eq. S6.2}$$

As for the covariate analysis, the identified SNPs, as well as patients' demographic information and clinical characteristics were considered. For continuous covariates, for each patient the mean values of all measurements during the monitoring period were taken. In case of missing continuous covariates, the corresponding median value of all patients was assigned. For patients who only missed HT but not WT, LBW was calculated using real WT and imputed HT. For GFR, 0 (normal) was assigned if ≥ 50% of the collected patient's records were 0 otherwise 1 was assigned. Patients who missed GFR measurements, 0 was assigned.

The effect of all above covariates on mitotane CL/F and the effect of WT, LBW, FAT, and gender on apparent distribution volumes (V/F) were investigated using stepwise covariate modelling (SCM) function implemented with Perl-Speaks-NONMEM (version 4.7.0) [1]. Both a forward inclusion ($p < 0.05$) and a backward elimination process ($p < 0.01$) were performed to identify significant covariates. For SNPs that were in 100% linkage disequilibrium, if they were included during the SCM analysis, the more clinically relevant ones would be selected in the final model. The effects of continuous covariates were investigated with both linear relation (Eq. S6.3) and power relation (Eq. S6.4), where P_i represents the parameter of *i*th individual, P_t represents typical value of the parameter, and η_i represents the individual variability, θ_{COV} represents the estimate of covariate effect, COV_i represents the covariate value of *i*th individual, COV_m is the median value of the covariate. Categorical covariates were analyzed with Eq. S6.5, where θ_{COV} was set as 1 for reference category and was estimated for other categories.

$$P_i = P_t \cdot (1 \pm \theta_{COV} \cdot (COV_i - COV_m)) \cdot e^{\eta_i} \quad \text{Eq. S6.3}$$

$$P_i = P_t \cdot (\frac{COV_i}{COV_m})^{\theta_{COV}} \cdot e^{\eta_i} \quad \text{Eq. S6.4}$$

$$P_i = P_t \cdot \theta_{COV} \cdot e^{\eta_i} \quad \text{Eq. S6.5}$$

Supplementary model evaluation methods

pcVPC was performed by 1000 times of simulation and the data points, 5th, 50th, and 95th percentiles of prediction-corrected observations were plotted together with 95% confidence intervals (CI) of 5th, 50th, and 95th percentiles of simulations. NPDE evaluation was performed with npde package (version 2.0) implemented in R statistics software based on 1000 times of simulations. The bootstrap was conducted by 1000 runs of bootstrap replicates sampled from original dataset with replacement, which was stratified on whether the subject contributed more than two data points after the end of treatment. The median as well as 95% CI of parameters were derived and compared with original parameter estimates.

Supplementary simulation method

Based on the final model structure, simulations were performed to evaluate different designed treatment strategies and approaches of starting dose determination. Patients were assumed to receive treatment as long as their last mitotane concentration monitoring time. The blood samples were assumed to be collected once every 2 weeks after knowing the result of the last sample, and the concentration of mitotane was assumed to be known 7 days after blood collection, which is in accordance with the optimal scenario in the clinical practice. The dose amount was subsequently adjusted accordingly.

As a comparison, a previous recommended 'high-dose' starting regimens, where the mitotane dose starts with 1.5 g per day and increases up to 6 g per day in 4 days, were simulated (**Regimen 1**) [2].

As for the newly designed regimens, the starting dose was 1) set as 2 g, 4 g, or 6 g for all patients according to the guideline [3] (**Regimen 2, 4, and 6**) or 2) set individually considering patients' characteristics with the help of the model (**Regimen 3, 5, 7, and 8**). As the expected time to reach the therapeutic target of mitotane is 3 to 5 months, the individually starting daily mitotane dose was estimated as the dose that allows the predicted mitotane concentrations on day 98 (C_{sim_pred98}) reach the therapeutic target. The C_{sim_pred98} was obtained by performing simulation under a regimen of 6 g per day increasing by 0 g (**Regimen 8**), 0.5 g (**Regimen 2, 3, 4, 5, 6–1, and 7–1**), or 1 g (**Regimen 6–2 and 7–2**) once every 21 days till the 98th day of treatment, with only typical parameter values and covariate effects considered. Given the linear PK feature of mitotane, the suggested starting daily dose (*Dose*) was therefore determined by Eqs. S6.6 and S6.7, where $\lceil X \rceil$ represents the least integer greater than or equal to X, $\lfloor X \rfloor$ represents the greatest integer less than or equal to *X*. Determining the starting dose based on the C_{sim_pred} on day 77 and 119 were also used for comparison.

$$X = \frac{14\ \text{mg/L}}{C_{sim\_(i)pred}} \cdot 6\text{g} \qquad \text{Eq. S6.6}$$

$$Dose = \begin{cases} \lceil X \rceil, & X - \lfloor X \rfloor > 0.650 \\ \lfloor X \rfloor + 0.5, & 0.350 \leq X - \lfloor X \rfloor \leq 0.650 \\ \lfloor X \rfloor, & X - \lfloor X \rfloor < 0.350 \end{cases} \qquad \text{Eq. S6.7}$$

Besides the above regimens, since individual parameters could be estimated after knowing one TDM result, **Regimen 9** was also designed and evaluated. In this strategy, patients were assumed to start with 4 g per day until the first TDM result was obtained. C_{sim_real} of each patient on day 14 was simulated, based on which the η_{IIVi} and η_{IOVi} were estimated for each patient using NONMEM with the POSTHOC function. Subsequently, the next daily dose of each patient was determined with Eqs. S6.6–S6.7 according to the individual C_{sim_pred98} ($C_{sim\_ipred98}$) under the daily dosing of 6 g, based on the model incorporating η_{IIVi} as was suggested in a previous study [4]. The constant starting regimen was applied in this regimen.

In **Regimen 2 to 8**, the dose increasing amount when C_{sim_real} < 14 mg/L was set differently before and after the target was reached (starting and maintenance regimen), in order to limit the toxicity at start and maintain the mitotane trough concentration within the therapeutic range at a later phase. The combination of 0 g/1.5 g, 0.5 g/1.5 g, 0.5 g/1 g, and 1 g/1.5 g were simulated and evaluated. **Regimen 2 to 7** applied stepwise increasing starting regimen and **Regimen 8** applied constant starting regimen. A maximum number of days

that follows the starting regimen was set as 126 (around 4 months) and 105 (98+7 days) for the stepwise increasing or constant starting regimens, respectively.

When C_{sim_real} reached 20 mg/L, a 50% dose reduction was suggested in **Regimen 1**. In comparison, both fixed dose amount reduction (3 g or 4 g) and 50% reduction were evaluated in the newly designed regimens (**Regimen 2 to 9**). If a reduction resulted in a dose level lower than 0 g, then 0 g was applied. Besides, an additional concentration threshold of dose reduction, 18 mg/L, with 1 g dose reduction was introduced in **Regimen 2 to 9**, since a 7-day period of no dose adjustment presented.

Supplementary References

1. Jonsson EN, Karlsson MO. Automated covariate model building within NONMEM. Pharm Res. 1998;15(9):1463-8. doi:10.1023/a:1011970125687.
2. Kerkhofs TM, Baudin E, Terzolo M, Allolio B, Chadarevian R, Mueller HH, et al. Comparison of two mitotane starting dose regimens in patients with advanced adrenocortical carcinoma. J Clin Endocrinol Metab. 2013;98(12):4759-67. doi:10.1210/jc.2013-2281
3. Koninklijke Nederlandse Maatschappij ter bevordering der Pharmacie. Mitotaan. 2019 [cited 2019 28 Aug]; Available from: https://kennisbank.knmp.nl/article/Informatorium_Medicamentorum/S1853.html.
4. Abrantes JA, Jonsson S, Karlsson MO, Nielsen EI. Handling interoccasion variability in model-based dose individualization using therapeutic drug monitoring data. British journal of clinical pharmacology. 2019;85(6):1326-36. doi:10.1111/bcp.13901.

Supplementary Tables

Table S6.1: Potential SNPs out of the 959 SNPs that are correlated to mitotane clearance based on the association analysis

	Gene	Common name	dbSNP.RS.ID	*P* value
1	*CYP2C18*	CYP2C18_c.1154C>T(T385M)	rs2281891	0.020
2	*CYP2C19*	CYP2C19*2_19154G>A(P227P)	rs4244285	0.020
3	*SLCO1B3*	SLCO1B3_c.334G>T(A112S)	rs4149117	0.027
4	*SLCO1B3*	SLCO1B3_c.699A>G(I233M)	rs7311358	0.027
5	*SLCO1B3*	SLCO1B3_c.1557G>A(A519A)	rs2053098	0.027
6	*SLCO1B1*	SLCO1B1_c.571T>C(L191L)	rs4149057	0.020
7	*VKORC1*	VKORC1_c.*134G>A(3'UTR)	rs7294	0.050
8	*VKORC1*	VKORC1_c.283+124G>C	rs8050894	0.030
9	*VKORC1*	VKORC1_c.174-136C>T	rs9934438	0.030
10	*VKORC1*	VKORC1_c.-1639G>A(Promoter)	rs9923231	0.030
11	*UGT1A6*	UGT1A6_c.315A>G(L105L)	rs1105880	0.042

Table S6.2: Additional potential SNPs that are correlated to mitotane clearance based on the association analysis, if the pre-set selection based on a translation file as recommended by Affymetrics® was not considered

	Gene	Common name	dbSNP.RS.ID	*P* value
1	*CA5P*	CA5P_A>G(rs11859842)	rs11859842	0.029
2	*SLC16A1*	SLC16A1_c.*1942T>C	rs9429505	0.0067
3	*CHST10*	CHST10_c.*381G>A	rs1530031	0.040
4	*CYP20A1*	CYP20A1_50767C>T(L346F)	rs1048013	0.014
5	*SLC22A13*	SLC22A13_c.*8336G>A	rs4679028	0.032
6	*UGT2A1*	UGT2A1_c.1305-109A>C	rs2288741	0.042
7	*ADH6*	ADH6_c.-930T>C	rs10002894	0.012
8	*ADH6*	ADH6_c.-2874T>C	rs6830685	0.012
9	*SLCO5A1*	SLCO5A1_c.97C>T(L33F)	rs3750266	0.015

Supplementary Figures

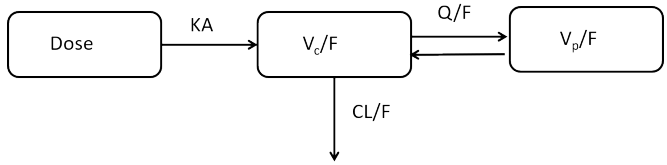

Figure S6.1: The population PK model structure of mitotane. CL/F represents apparent system clearance, KA represents absorption rate constant, V_c/F represents apparent distribution volume of central compartment, V_p/F represents apparent distribution volume of peripheral compartment, Q/F represents apparent distribution rate constant.

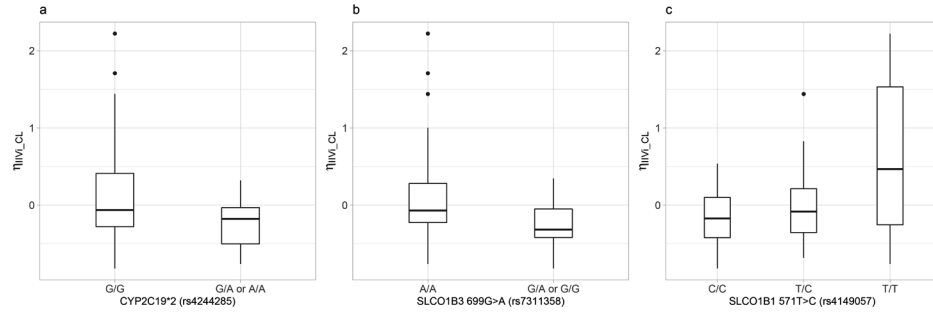

Figure S6.2: The boxplots of estimated η_{IIVi_CL} in each genotype group of SNP **(a)** CYP2C19*2 (rs4244285), **(b)** SLCO1B3 699A>G (rs7311358), and **(c)** SLCO1B1 571T>C (rs4149057).

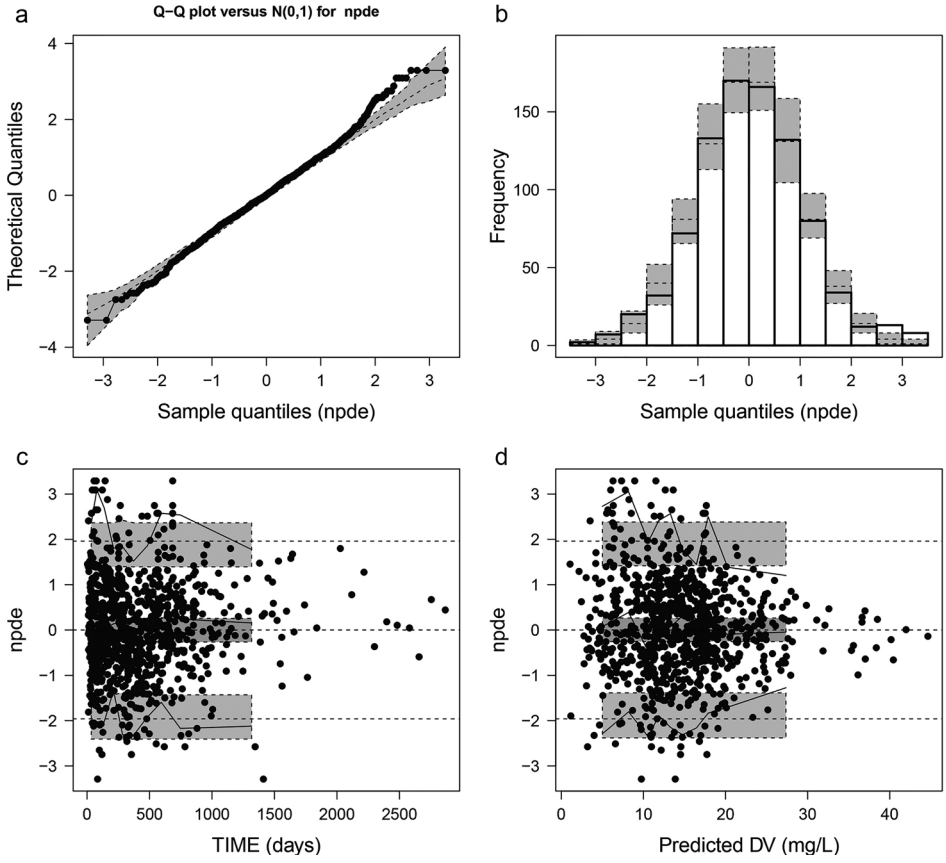

Figure S6.3: Normalized prediction distribution error (NPDE) results of the final population PK model of mitotane in patients with ACC, including the quantile–quantile plot **(a)**, the distribution histogram of NPDE **(b)**, and the NPDE versus time **(c)** and population predictions **(d)**. The NPDE results are shown to distribute around a mean of 0.03616 with a variance of 1.134.

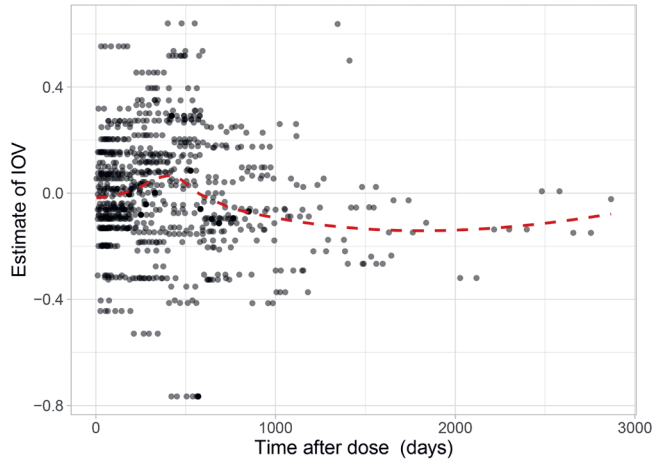

Figure S6.4: The estimates of inter-occasion variability (IOV) over time. Red dashed lines represent loess regression result.

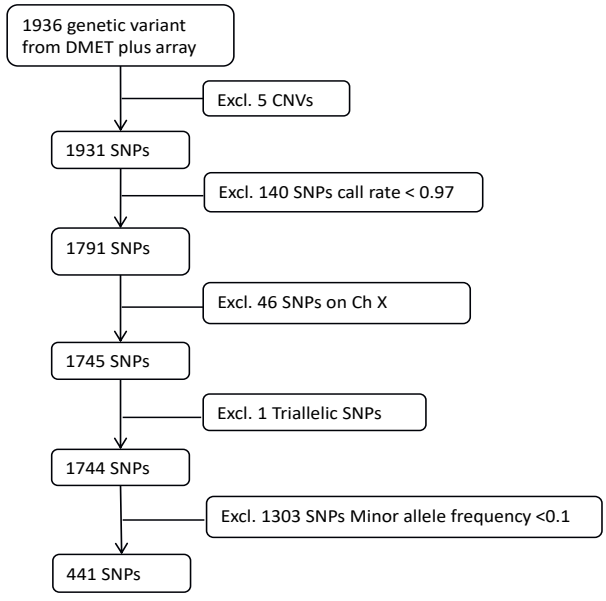

Figure S6.5: Flow diagram of the genetic variants selection if the pre-set selection based on a translation file as recommended by Affymetrics® was not considered. Excl. represents excluding, Ch X represents chromosome X, DMET™ represent Drug Metabolizing Enzymes and Transporters, CNVs represents copy number variations.

Online Resource 6.2: Shiny app establishing method and results

Shiny app establishment

Based on the final mitotane population pharmacokinetic model, a Shiny app was established for the simulation for a random patient and to elucidate an example of the model application on guiding treatment for a new patient. Package shiny (version 1.4.0) and RxODE (version 0.6-1) in R statistics software (version 3.4.2; R Foundation for Statistical Computing, Vienna, Austria) were utilized. The R script can be found through: https://github.com/AnyueYin/Shiny-app-script-for-model-simulation---Population-PK-and-PG-analysis-of-mitotane. Patient gender, weight, and height, which were used to estimate lean body weight (LBW) and fat amount (FAT), as well as the results of three SNPs were in the input panel, based on which the starting dose was suggested. One hundred times of simulation under an optimized mitotane treatment regimen, Regimen 5–(– 4 g), were performed given the input information. The 90% prediction interval, 50th percentile of the predictions, target reaching time, and suggested starting dose were plotted in the output figure. The residual errors were not considered in the simulation.

Screen shots of the developed shiny app is shown in **Figure S6.6**. The result shows that for a male patient with 85 kg weight and 180 cm height who carries G/G, A/A, and T/C for *CYP2C19*2* (rs4244285), *SLCO1B3* 699A>G (rs7311358), and *SLCO1B1* 571T>C (rs4149057), respectively, the 90% prediction interval can nicely locate within the therapeutic window of mitotane. The starting dose was suggested as 5.5 g per day and the 50th percentile of the predictions reached the target on day 92. If the genotype result of *CYP2C19*2* (rs4244285) changed to G/A, the suggested starting dose became 4 g per day and the 50th percentile of the predictions reached the target on day 94.

In addition, a model with FAT effect on central distribution volume as the only covariate (**Table S6.3**) was also built in the Shiny app as an alternative option to allow dosing advice and concentration prediction for patients when genotyping results are not available (**Figure S6.6c**).

Table S6.3: Parameter estimates of the final model without genotyping results as covariates

	Final model		
Parameters	Estimate (RSE%)	IIV (CV%) [shrinkage, %]	IOV[a] (CV%)
KA (/day)	15.0 fixed	-	-
CL/F (L/day)	217 (9)	66.3 [7]	31.2
V_c/F (L)	8450 (16)	63.5 [37]	-
V_c_FAT (power)	1.12 (18)	-	-
V_p/F (L)	15500 (15)	80.4 [36]	-
Q/F (/day)	609 (28)	100.5 [38]	-
Residual errors			
PRO (CV%)	16.7 (6)	-	-
ADD (mg/L)	0.907 (16)	-	-

FAT, fat amount; RSE, relative standard error; CV, coefficient of variation; IIV, inter-individual variability; IOV, inter-occasion variability; PRO, proportional residual error; ADD, additive residual error; CL/F, apparent system clearance; KA, absorption rate constant; V_c/F, apparent distribution volume of central compartment; V_p/F, apparent distribution volume of peripheral compartment; Q/F, apparent distribution rate constant.
[a] Every 200 days of dosing was defined as an occasion.

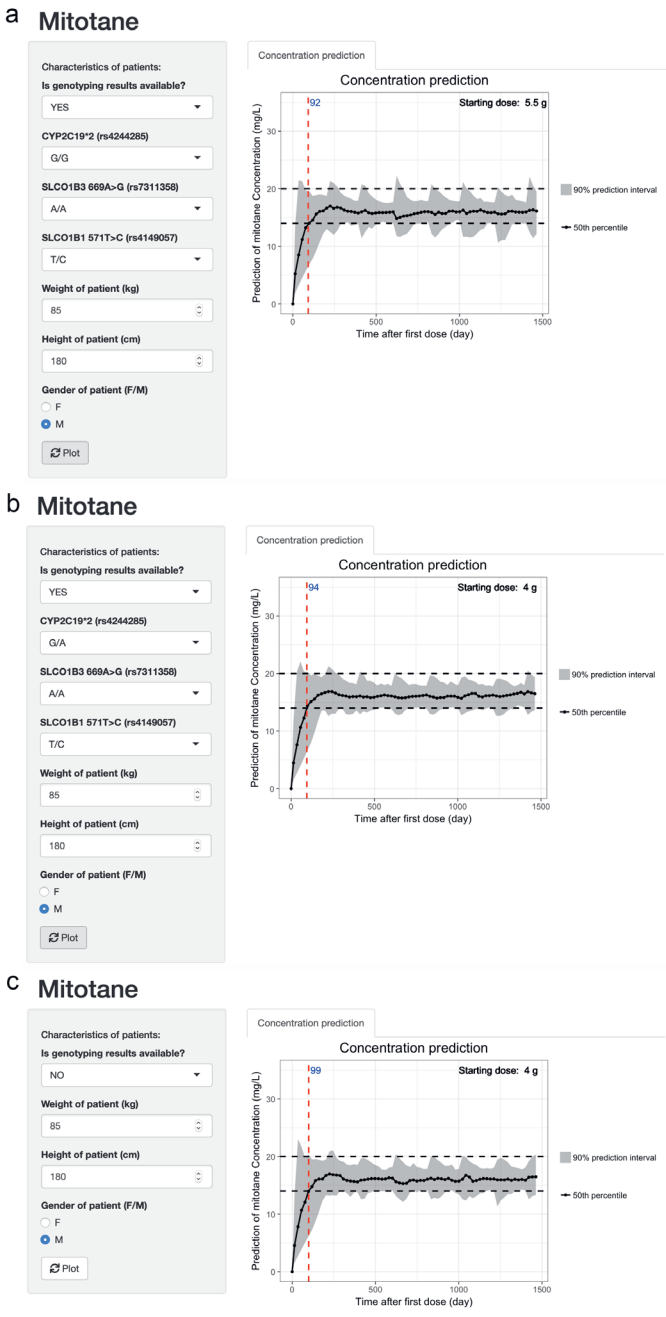

Figure S6.6: Screen shot of the shiny app established based on the final model. **(a)** A male patient with 85 kg weight and 180 cm height who carries G/G, A/A, and T/C for *CYP2C19*2* (rs4244285), *SLCO1B3* 699A>G (rs7311358), and *SLCO1B1* 571T>C (rs4149057), respectively. **(b)** A male patient with 85 kg weight and 180 cm height who carries G/A, A/A, and T/C for *CYP2C19*2* (rs4244285), *SLCO1B3* 699A>G (rs7311358), and *SLCO1B1* 571T>C (rs4149057), respectively. **(c)** A male patient with 85 kg weight and 180 cm height whose genotyping results are unknown.

Online Resource 6.3: List of 959 SNPs from DMET™ array of which the genotyping results were obtained for each patient

The online version of this article (https ://doi.org/10.1007/s4026 2-020-00913 -y) contains this supplementary material, which is available to authorized users.